Chinese Chemical Letters 33 (2022) 2081–2085

Contents lists available at ScienceDirect

Chinese Chemical Letters

journal homepage: www.elsevier.com/locate/cclet

Fluorescent MOF-based nanozymes for discrimination of phenylenediamine isomers and ratiometric sensing of *o*-phenylenediamine

Yinghui Xia, Kunming Sun, Ya-Nan Zuo, Shuyun Zhu*, Xian-En Zhao*

School of Chemistry and Chemical Engineering, Qufu Normal University, Qufu 273165, China

ARTICLE INFO

Article history:
Received 22 June 2021
Revised 19 July 2021
Accepted 17 August 2021
Available online 22 August 2021

Keywords:
Bifunctional MOF
Nanozyme
Photoluminescence
Aromatic diamine isomers
Ratiometric fluorescence

ABSTRACT

Although peroxidase-like nanozymes have made great progress in bioanalysis, few current nanozyme-based biosensors are constructed for discriminating isomers of organic compounds. Herein, fluorescent metal-organic framework (MOF)-based nanozyme is utilized for phenylenediamine isomers discrimination and detection. NH_2-MIL-101(Fe), as a member of Fe-based MOFs, functions as not only fluorescent indicator but also peroxidase mimics. In the presence of H_2O_2, NH_2-MIL-101(Fe) can catalyze the oxidation of o-phenylenediamine (OPD) and p-phenylenediamine (PPD) into their corresponding oxidation products (OPDox and PPDox), which in turn quench its intrinsic fluorescence at 445 nm *via* inner filter effect (IFE). Differently, a new fluorescence peak at 574 nm is observed for OPDox. Thus, a ratiometric fluorescence method for the detection of OPD can be designed with the fluorescence intensity ratio F_{574}/F_{445} as readout. This proposed strategy displays excellent discrimination ability for three phenylenediamines and may open new applications of MOFs in environmental science.

Bifunctional NH_2-MIL-101(Fe) was utilized for phenylenediamine isomers discrimination and detection for the first time.

Discriminating structural isomers of organic compounds have always been a challenging task in environmental fields because they possess similar physical and chemical properties resulting from the subtle distinctions in the structures [1–3]. *o*-Phenylenediamine (OPD), *m*-phenylenediamine (MPD), and *p*-phenylenediamine (PPD) are three isomers of phenylenediamines that have been used as precursors in various fields including plastics production, pharmaceuticals and industrial dyes [4,5]. However, their damages to the human health and environment upon prolonged exposure are different. OPD is a highly toxic and carcinogenic environmental pollutant [6,7]. PPD can cause various immediate allergic reactions [8]. MPD does not lead to obvious harmful effects. A number of methods have been applied for the discrimination of phenylenediamines such as chromatography [9,10], chromatography-mass spectrometry [11,12] and capillary electrophoresis [13]. These approaches can realize the detection of three phenylenediamines at the same time, but they need complicated sample pretreatments and high operation cost.

As an alternative, fluorescence strategies have drawn wide interest owing to their simplicity, easy operation and high sensitivity [14,15]. For example, Lai and coworkers synthesized the fluorescent quinoxaline through a tandem reaction for the detection of OPD [16]. Ngeontae's group designed a fluorometric sensor for PPD based on alizarin-boronic acid adduct [17]. Wang's group constructed a fluorescent sensor for PPD on the basis of amine-aldehyde condensation reaction by using 1-pyrenecarboxaldehyde as a probe [18]. Although these methods exhibit high sensitivity, they analyze only one phenylenediamine isomer. It still remains a great challenge to design a fluorescence strategy for the identification and detection of the three phenylenediamines. Moreover, these strategies are based on single signal output, and the results are influenced easily by excitation light source and external environmental conditions. Fortunately, the ratiometric fluorescent strategy, which is based on dual-signal measurement simultaneously, can overcome such drawbacks [19,20]. Fluorescent nanomaterials hold great promise to construct ratiometric assays [21–23]. Generally speaking, most nanoprobe-based ratiometric systems are composed of two different kinds of nanoprobes. Undoubtedly, the synthesis procedures for two different kinds of nanomaterials are complex and time-consuming. Thus, some scientists shift their focus to the design and synthesis of bifunctional fluorophores.

* Corresponding authors.
E-mail addresses: shuyunzhu1981@163.com (S. Zhu), xianenzhao@163.com (X.-E. Zhao).

https://doi.org/10.1016/j.cclet.2021.08.083
1001-8417/

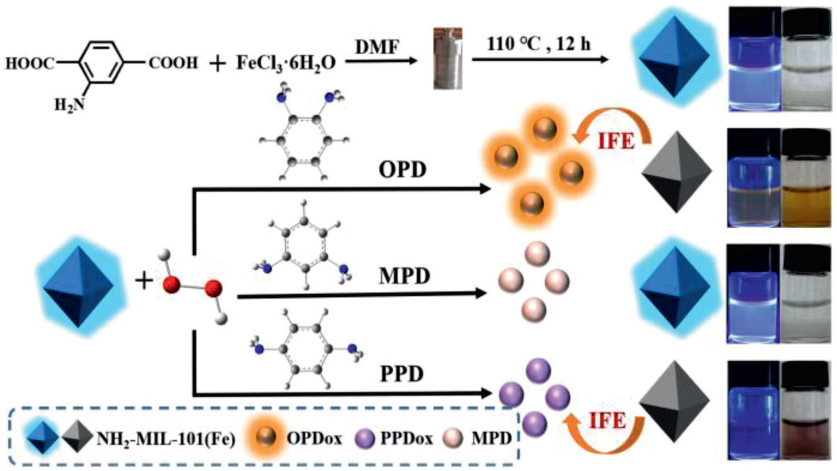

Fig. 1. Discrimination of phenylenediamine isomers based on fluorescent NH_2-MIL-101(Fe)-based nanozyme.

Fluorescent nanozymes can function as not only fluorescence reporters but also peroxidase mimics, which can catalyze the oxidation of nonfluorescent substate into luminophore with the assistance of H_2O_2. Thus, these fluorescent nanozymes combined with substrate of peroxidase can display dual-emission with single excitation. Up to date, various fluorescent nanozymes including functional carbon dots (CDs) [24], graphitic carbon nitride (C_3N_4) [25,26], gold nanoclusters (AuNCs) [27] and copper nanoclusters (CuNCs) [28] have been used to construct ratiometric assays. However, the research about fluorescent nanozymes is in the embryo stage. It is necessary to design novel fluorescent nanozymes and apply them in ratiometric sensing.

Metal-organic frameworks (MOFs) are highly porous materials assembled by metal clusters and organic ligands which endow them with multiple functions [29–31]. The usage of organic ligands can make MOFs attractive optical properties while the unsaturated metallic nodes allow MOFs to exhibit excellent biomimetic catalytic activity [32,33]. It has been reported that NH_2-MIL-101(Fe) exhibits two functions, in which the 2-aminoterephthalic acid ligand (1,4-BDC-NH_2) and Fe node make the framework a blue photoluminescence and peroxidase-mimetic catalytic activity, respectively. Bifunctional NH_2-MIL-101(Fe)-based ratiometric fluorescence assays for pesticide [34] and acid phosphatase activity [35] have been developed. However, no fluorescence sensor has been developed for discriminating phenylenediamine isomers and ratiometric detection of OPD with bifunctional NH_2-MIL-101(Fe).

Here, we fabricate a fluorescence sensing platform to discriminate three aromatic amines (OPD, MPD, and PPD) and detect OPD ratiometrically with bifunctional MOF (Fig. 1). The NH_2-MIL-101(Fe) exhibits an intrinsic fluorescence at 445 nm ascribed to 1,4-BDC-NH_2 linker. Simultaneously, the Fe-O clusters endow NH_2-MIL-101(Fe) with peroxidase-like activity to activate H_2O_2 to produce $^{\bullet}OH$ radicals, which oxidize colorless OPD into its oxidized products (OPDox) with strong fluorescence emission at 574 nm. The generated OPDox can in turn quench the fluorescence of NH_2-MIL-101(Fe) *via* inner filter effect (IFE). With F_{574}/F_{445} as readout, OPD can be detected ratiometrically. PPD can be oxidized by produced $^{\bullet}OH$ to its oxidized form (PPDox), which just quenches the fluorescence of NH_2-MIL-101(Fe) *via* IFE without the generation of new emission peak. The introduction of MPD cannot induce obvious change for the fluorescence of NH_2-MIL-101(Fe). Thus, OPD, MPD and PPD can be discriminated effectively with fluorescent NH_2-MIL-101(Fe)-based nanozyme.

NH_2-MIL-101(Fe) was synthesized by typical solvothermal process according to the previous paper [34,35]. The preparation process of NH_2-MIL-101(Fe) can be found in Supporting Information. Fig. 2A shows the X-ray diffraction (XRD) characteristic peaks of the obtained NH_2-MIL-101(Fe) are in agreement with a simulation of MIL-101 [36]. Scanning electron microscopy (SEM) image shows that NH_2-MIL-101(Fe) displays a typical octahedral morphology with a diameter around 400 nm (Fig. 2B). Fig. S1 (Supporting information) shows the FT-IR spectra of both NH_2-MIL-101(Fe) and 1,4-BDC-NH_2. Two peaks at 3400 cm^{-1} are observed ascribed to symmetrical and asymmetrical stretching vibrations of amine [37]. The peak at 1651 cm^{-1} indicates the presence of carboxyl group. In comparison with ligand, a peak at 571 cm^{-1} indicates the existence of Fe-O bond in MOFs. The full X-ray photoelectron spectra (XPS) shows that NH_2-MIL-101(Fe) is composed of Fe, N, O and C (Fig. 2C). The Fe 2p XPS indicates that the Fe element is composed of Fe^{2+} and Fe^{3+} (Fig. 2D). This Fe^{3+}/Fe^{2+} redox endows NH_2-MIL-101(Fe) with peroxidase-like activity [34].

It is supposed that NH_2-MIL-101(Fe) is photoluminescent ascribed to the ligand. As expected, NH_2-MIL-101(Fe) exhibits a strong fluorescence at 445 nm which is consistent with that of 1,4-BDC-NH_2 (Fig. S2A in Supporting information). The results indicate that the fluorescence property of NH_2-MIL-101(Fe) derives from ligand. Moreover, the fluorescence emissions of NH_2-MIL-101(Fe) under different excitation wavelengths were investigated. The fluorescence intensity decreases gradually with increasing excitation wavelengths from 360 nm to 400 nm (Fig. S2B in Supporting information), which is consistent with the previous report [34]. The feasibility for discriminating phenylenediamines with fluorescent NH_2-MIL-101(Fe)-based nanozymes was examined. As presented in Fig. 3A, only NH_2-MIL-101(Fe) exhibits a blue emission at 445 nm upon exciting at 375 nm (curve a, vial a). After introducing H_2O_2 and OPD, the emission signal at 445 nm decreases while a new emission ascribed to OPDox appears at 574 nm (curve b). The solution exhibits orange-yellow fluorescence under ultraviolet light (vial b). The emission at 445 nm is quenched obviously without the appearance of new peak with H_2O_2 and PPD (curve c, vial c). However, the introduction of H_2O_2 and MPD causes slight change for the emission of NH_2-MIL-101(Fe) (curve d, vial d). In contrast, the emission signals of MOF keep almost unchanged with any phenylenediamines (Fig. S3 in Supporting information).

UV-vis absorption spectra were studied to further prove the discrimination of phenylenediamines with NH_2-MIL-101(Fe)-based nanozymes (Fig. 3B). Upon the addition of H_2O_2, a weak absorption peak at 435 nm for OPD and 490 nm for PPD is observed, corresponding to OPDox and PPDox, respectively. In contrast, there is no obvious absorption peak for MPD with the coex-

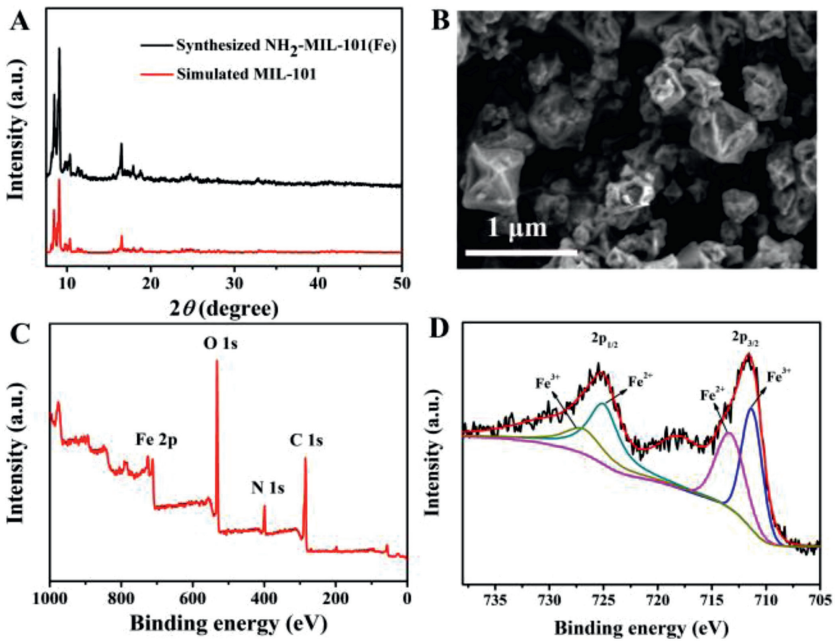

Fig. 2. (A) XRD profiles of NH_2-MIL-101(Fe) and simulated MIL-101(Fe). (B) SEM image of NH_2-MIL-101(Fe). (C) and (D) show the full XPS and Fe 2p XPS of NH_2-MIL-101(Fe), respectively.

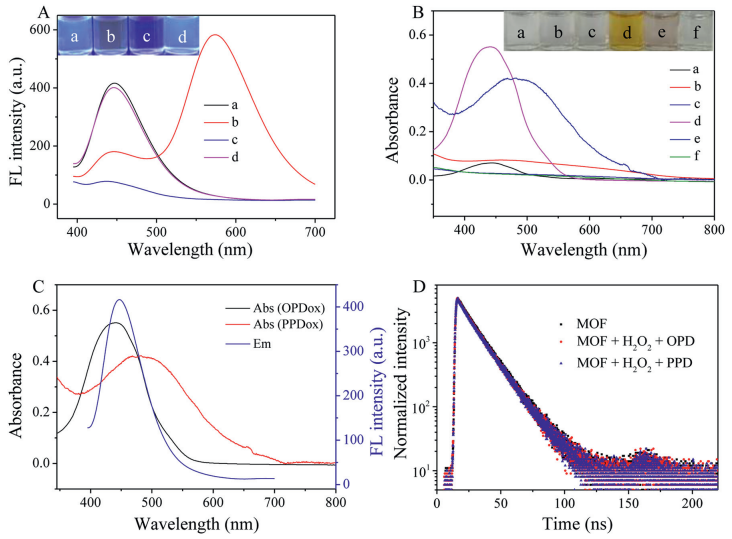

Fig. 3. (A) Fluorescence emission spectra of NH_2-MIL-101(Fe) (a) and NH_2-MIL-101(Fe) in the presence of H_2O_2 and OPD (b), H_2O_2 and PPD (c), and H_2O_2 and MPD (d). Inset: the corresponding photos under ultraviolet light. (B) UV-vis spectra of H_2O_2 + OPD (a), H_2O_2 + PPD (b), H_2O_2 + MPD (c), H_2O_2 + OPD + NH_2-MIL-101(Fe) (d), H_2O_2 + PPD + NH_2-MIL-101(Fe) (e) and H_2O_2 + MPD + NH_2-MIL-101(Fe) (f). Inset: the corresponding photos under daylight. (C) UV-vis absorption spectra of OPDox as well as PPDox and emission spectrum of NH_2-MIL-101(Fe) under the excitation wavelength of 375 nm. (D) PL decay of NH_2-MIL-101(Fe) in the absence and presence of H_2O_2-OPD and H_2O_2-PPD.

istence of H_2O_2. Furthermore, when NH_2-MIL-101(Fe) coexists with OPD + H_2O_2/PPD + H_2O_2, absorbance at both 435 nm and 490 nm increases remarkably. However, there is no obvious absorption in the systems of NH_2-MIL-101(Fe) + OPD, NH_2-MIL-101(Fe) + PPD, NH_2-MIL-101(Fe) + MPD and NH_2-MIL-101(Fe) + H_2O_2 (Fig. S4 in Supporting information). These results indicated NH_2-MIL-101(Fe) can catalyze the oxidation of OPD and PPD easily with the assistance of H_2O_2 [38,39]. Experiments were performed to further prove the generation of hydroxyl radicals (•OH) during the catalytic oxidation. As a scavenger for •OH radicals, thiourea is added into the NH_2-MIL-101(Fe)- H_2O_2-OPD system. As presented in Fig. S5 (Supporting information), the emission signal at 574 nm decreases gradually with the increasing concentration of thiourea, showing that •OH is indeed produced in this system and involves in phenylenediamine oxidation reaction. All the results further indicate that the three phenylenediamines can be discriminated with fluorescent NH_2-MIL-101(Fe)-based nanozymes.

Then, we investigated the response mechanism of NH_2-MIL-101(Fe)-H_2O_2 system for phenylenediamines. As presented in Fig. 3C, the absorption spectra of both OPDox and PPDox exhibit a large overlap with the emission spectrum of NH_2-MIL-101(Fe). Furthermore, the fluorescent lifetime (τ) measurements were performed to investigate their interaction with the results exhibited in Fig. 3D. The fluorescence decay profile of NH_2-MIL-101(Fe) changes slightly with OPDox/PPDox. The τ of NH_2-MIL-101(Fe) in the absence and presence of OPDox and PPDox is 14.1 ± 0.24 ns, 13.77 ± 0.37 ns and 13.68 ± 0.25 ns, respectively. Thus, energy or electron transfer is excluded. All the above results meet the conditions

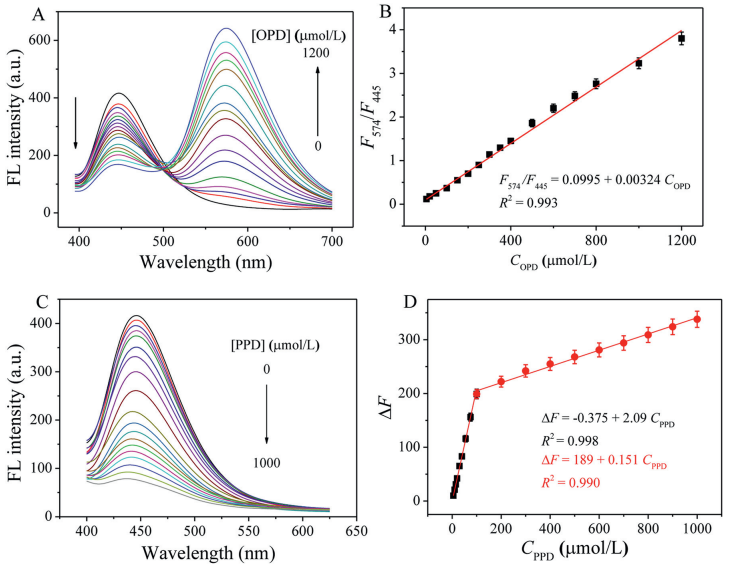

Fig. 4. (A) Fluorescence emission spectra of NH_2-MIL-101(Fe)-H_2O_2 system with varied concentrations of OPD (0, 5, 20, 50, 100, 200, 250, 300, 350, 400, 500, 600, 700, 800, 1000, 1200 μmol/L). (B) Linear relationship between F_{574}/F_{445} and OPD concentration. (C) Fluorescence emission spectra of NH_2-MIL-101(Fe)-H_2O_2 system with varied concentrations of PPD (0, 5, 10, 15, 20, 30, 40, 55, 75, 100, 200, 300, 400, 500, 600, 700, 800, 900, 1000 μmol/L). (D) Linear relationship between ΔF and PPD concentration.

of inner filter effect (IFE). Therefore, we conclude that NH_2-MIL-101(Fe) is quenched by OPDox/PPDox *via* IFE.

To improve the sensitivity of this assay for OPD, several factors such as reaction time, pH, concentration of H_2O_2 and amount of NH_2-MIL-101(Fe) were optimized. The best reaction time, pH, concentration of H_2O_2 and amount of NH_2-MIL-101(Fe) is 60 min, 5.0, 20 mmol/L, and 0.5 μg/mL, respectively (Fig. S6 in Supporting information). Under optimal conditions, with the increasing concentration of OPD, the emission signals at 445 nm decrease whereas those at 574 nm increase (Fig. 4A). The F_{574}/F_{445} is proportional to the concentration of OPD from 5 μmol/L to 1200 μmol/L with the regression equation of $F_{574}/F_{445} = 0.0995 + 0.00324\ C_{OPD}$ ($R^2 = 0.993$) (Fig. 4B). The limit of detection (LOD) is calculated to be 1.5 μmol/L (S/N = 3). Similarly, the fluorescence at 445 nm decreases gradually when PPD concentration increases (Fig. 4C). With the $\Delta F = F_0 - F$ (F_0 and F is the fluorescence intensity of NH_2-MIL-101(Fe)-H_2O_2 system without and with PPD, respectively) as readout, two linear calibration curves are achieved for PPD in the range of 5-100 μmol/L ($R^2 = 0.998$) and 100-1000 μmol/L ($R^2 = 0.990$), respectively (Fig. 4D). The LOD for PPD is calculated to be 1.0 μmol/L (S/N = 3). Compared with colorimetric methods for discriminating phenylenediamine isomers, this fluorescent method has wider linear range and lower LOD [39,40] (Table S1 in Supporting information). Moreover, most fluorescent methods can detect only one phenylenediamine [4,16,17,41] while this strategy can realize the detection of OPD and PPD (Table S1).

The reproducibility of this assay was investigated by repetitive analysis of OPD and PPD at the identical and different batches. The relative standard deviations (RSDs) of the intra-assay were 2.34% (n = 5) for 0.5 mmol/L OPD and 3.12% (n = 5) for 0.5 mmol/L PPD at the same-batch sensors. The batch-to-batch reproducibility was also investigated by six parallel prepared NH_2-MIL-101(Fe). The RSDs were 4.6% and 5.1% for 0.5 mmol/L OPD and 0.5 mmol/L PPD, respectively. These results demonstrate the satisfactory reproducibility of the designed assay. In addition, the stability of this assay was evaluated. The fluorescence responses of NH_2-MIL-101(Fe) towards OPD and PPD with the same concentration (0.5 mmol/L) were recorded after the NH_2-MIL-101(Fe) was kept at 4 °C for 60 days. The assay retains 97% and 95% of its initial responses for OPD and PPD, respectively, indicating that this assay exhibits good stability.

To examine the selectivity of this strategy for sensing OPD and PPD, control experiments were carried out using potential interferences including Fe^{3+}, Ca^{2+}, Zn^{2+}, NO_3^-, SO_4^{2-}, tryptophan (Trp), tyrosine (Tyr), phenylalanine (Phe), ascorbic acid (AA), glutathione (GSH), cysteine (Cys), phenol, 3-nitrophenol (3-NP), 4-aminophenol (4-AP), catechol (CC), resorcinol (RC), hydroquinone (HQ), benzaldehyde (BA), aniline, melamine (MA), MPD. As presented in Fig. S7A (Supporting information), these interferences cause negligible changes for F_{574}/F_{445} while the F_{574}/F_{445} increases greatly in the presence of OPD. Interference experiments were also performed with the results shown in Fig. S7B (Supporting information). F_{574}/F_{445} values for OPD detection remain unchanged in the presence of potential interferences except PPD. Fig. S7C (Supporting information) shows that the ΔF values caused by these interferences are much lower than that of PPD. Similarly, the interference experiments show that ΔF values for PPD detection change negligibly with potential interferences except OPD. Overall, these results demonstrate that the bifunctional NH_2-MIL-101(Fe)-based fluorescent assays exhibit an acceptable selectivity towards OPD and PPD. Nevertheless, if OPD and PPD coexist in a sample, they interfere with each other for the detection.

To evaluate the practical performance of this strategy, OPD and PPD in Weishan Lake water were analyzed by standard addition method. The detailed analysis process was provided in Supporting information. As shown in Table S2 (Supporting information), the recoveries range from 94.4% to 106.9% for OPD and 93.6% to 96.2% for PPD with the RSD less than 4.0%, revealing the satisfactory reliability and accuracy. The results indicate that this method possesses the great promise in the real sample analysis.

In summary, we have demonstrated the usage of bifunctional NH_2-MIL-101(Fe) for phenylenediamine isomers discrimination and detection for the first time. The NH_2-MIL-101(Fe) not only exhibits an intrinsic blue fluorescence ascribed to the fluorescent ligand but also excellent peroxidase-mimic activity due to the presence of Fe node. With the assistance of H_2O_2, OPD and PPD can be oxidized by NH_2-MIL-101(Fe) into their corresponding products, which quench the fluorescence of NH_2-MIL-101(Fe) through IFE. In addition, a new emission at 574 nm emerges for OPDox. There-

fore, a ratiometric fluorescence assay for OPD is developed. The introduction of MPD cannot induce obvious change for the fluorescence of NH_2-MIL-101(Fe). Thus, the three phenylenediamines can be discriminated with NH_2-MIL-101(Fe)-H_2O_2 system. This fabricated nanosensor has been successfully utilized to identify OPD and PPD in water samples. Such a new strategy can enable fluorescence MOF-based nanozyme promising applications in environmental monitoring.

Declaration of competing interest

The authors declare that they have no known competing financial interests or personal relationships that could have appeared to influence the work reported in this paper.

Acknowledgments

This work is kindly supported by the National Natural Science Foundation of China (No. 22076097) and the Natural Science Foundation of Shandong Province (No. ZR2020MB066).

Supplementary materials

Supplementary material associated with this article can be found, in the online version, at doi:10.1016/j.cclet.2021.08.083.

References

[1] H.F. Wang, Y.Y. Wu, X.P. Yan, Anal. Chem. 85 (2013) 1920–1925.
[2] S. Samanta, C. Kar, G. Das, Anal. Chem. 87 (2015) 9002–9008.
[3] F. Wang, Y. Yang, T.M. Swager, Angew. Chem. Int. Ed. 44 (2008) 8522–8524.
[4] D. Mathivanan, S.K. Tammina, X.L. Wang, Y.L. Yang, Microchim. Acta 187 (2020) 292.
[5] B. Shi, J. Su, L. Zhang, et al., Nanoscale 8 (2016) 10814–10822.
[6] M. Matsumoto, M. Suzuki, H. Kano, et al., Arch. Toxicol. 86 (2012) 791–804.
[7] A. Nezamzadeh-Ejhieh, Z. Salimi, Appl. Catal. A 390 (2010) 110–118.
[8] M. Gu, J. Duan, Q.Q. Mao, S.H. Zhang, J.G. Lv, Sens. Actuators. B: Chem. 287 (2019) 173–179.
[9] H. Tokuda, Y. Kimura, S. Takano, J. Chromatogr. A 367 (1986) 345–356.
[10] S.P. Wang, T.H. Huang, Anal. Chim. Acta 534 (2005) 207–214.
[11] P.G. Wang, A.J. Krynitsky, J. Chromatogr. B 879 (2011) 1795–1801.
[12] P. Dobberstein, E. Korte, G. Meyerhoff, R. Pesch, Int. J. Mass Spectrom. Ion Processes 46 (1983) 185–188.
[13] S. Dong, L. Chi, S. Zhang, et al., Anal. Bioanal. Chem. 391 (2008) 653–659.
[14] F. Qu, Z.W. Guo, D.F. Jiang, X.E. Zhao, Chin. Chem. Lett. 32 (2021) 3368–3371.
[15] M. Li, B. Gurram, S. Lei, et al., Chin. Chem. Lett. 32 (2021) 1316–1330.
[16] X.J. Lai, G.Y.S. Qiu, Q.X. Ye, R.X. Wang, J.B. Liu, J. Photochem. Photobio. A 386 (2020) 112101.
[17] K. Ngamdee, S. Martwiset, T. Tuntulani, W. Ngeontae, Sens. Actuators B: Chem. 173 (2012) 682–691.
[18] L.F. Gao, X. Lin, X. Hai, X.W. Chen, J.H. Wang, ACS Appl. Mater. Interfaces 10 (2018) 43049–43056.
[19] L.Y. Liu, S.Y. Zhu, J. Sun, et al., Chin. Chem. Lett. 32 (2021) 906–909.
[20] M. Xia, X.E. Zhao, J. Sun, Z.J. Zheng, S.Y. Zhu, Sens. Actuators B: Chem. 319 (2020) 128321.
[21] Q.M. Qiu, H.Y. Chen, Y.X. Wang, Y.B. Ying, Coord. Chem. Rev. 387 (2019) 60–78.
[22] Y.Y. Li, Y.N. Ban, R.H. Wang, et al., Chin. Chem. Lett. 31 (2020) 443–446.
[23] M.K. Wang, D.S. Kong, D.D. Su, Y. Liu, S.G. Su, Nanoscale 11 (2019) 13903–13908.
[24] L.Z. Wang, Y. Liu, Z.P. Yang, et al., Dyes Pigm. 180 (2020) 108486.
[25] X.Y. Wang, L. Qin, M.J. Lin, H. Xing, H. Wei, Anal. Chem. 91 (2019) 10648–10656.
[26] W.F. Deng, Y. Peng, H. Yang, et al., ACS Appl. Mater. Interfaces 11 (2019) 29072–29077.
[27] Y.N. Qin, Y.J. Sun, Y.J. Li, et al., Chin. Chem. Lett. 31 (2020) 774–778.
[28] S. Maity, D. Bain, S. Chakraborty, S. Kolay, A. Patra, ACS Sustainable Chem. Eng. 8 (2020) 18335–18344.
[29] J.F. Chang, X. Wang, J. Wang, H.Y. Li, F. Li, Anal. Chem. 91 (2019) 3604–3610.
[30] J.F. Chang, W.X. Lv, Q. Li, H.Y. Li, F. Li, Anal. Chem. 92 (2020) 8959–8964.
[31] H. Wang, X.L. Wang, R.M. Kong, L. Xia, F.L. Qu, Chin. Chem. Lett. 32 (2021) 198–202.
[32] S.Q. Li, X.D. Liu, H.X. Chai, Y.M. Huang, TrAC Trends Anal. Chem. 105 (2018) 391–403.
[33] X.H. Niu, X. Li, Z.Y. Lyu, et al., Chem. Commun. 56 (2020) 1338.
[34] P. Liu, X. Liu, X.C. Xu, et al., Sens. Actuators B: Chem. 328 (2021) 129024.
[35] S.Q. Li, X. Hu, Q.M. Chen, et al., Biosens. Bioelectron. 137 (2019) 133–139.
[36] J.J. Guo, S. Wu, Y. Wang, M. Zhao, Sens. Actuators B: Chem. 312 (2020) 128021.
[37] Z.G. Zhang, X.Y. Li, B.J. Liu, Q.D. Zhao, G.H. Chen, RSC Adv. 6 (2016) 4289–4295.
[38] B.F. Shi, Y.B. Su, L.L. Zhang, et al., Nanoscale 8 (2016) 10814–10822.
[39] L.P. Lin, Y.L. Xiao, Y.H. Wang, et al., Microchim. Acta 186 (2019) 288.
[40] R. Maria-Hormigos, B. Jurado-Sanchez, A. Escarpa, Anal. Chem. 90 (2018) 9830–9837.
[41] Y.J. Zhao, K. Miao, Z. Zhu, L.J. Fan, ACS Sensors 2 (2017) 842–847.